Simulation of a frequency-reconfigurable multiband antenna for 5G and Wi-Fi 6E/7 applications

Ismahane Refsi[1], Miloud Benchehima[2], Mohammed Hicham Hachemi[3], Salah Eddine Brezini[4]
[1]Laboratory of Coding and Security of Information, Faculty of Electrical Engineering,
University of Sciences and Technology of Oran Mohamed Boudiaf, Oran, Algeria
[2]Applied Materials Laboratory, Research CENTER (CFTE), Djillali Liabes University, Sidi Bel Abbes, Algeria
[3]STIC Laboratory, Faculty of Technology, University of Tlemcen, Tlemcen, Algeria
[4]Signal and Image Laboratory, University of Sciences and Technology of Oran Mohamed Boudiaf, Oran, Algeria

Article Info

Article history:

Received Feb 6, 2026
Revised Apr 15, 2026
Accepted Jun 27, 2026

Keywords:

5G
CPW-fed
Frequency reconfigurable
Multiband
Wi-Fi 6E/7

ABSTRACT

This paper presents a compact frequency-reconfigurable multiband antenna design suitable for 5G and Wi-Fi 6E/7 applications. Designed on a low-cost FR4 substrate, the antenna occupies a compact footprint of 28×15×1.6 mm, making it one of the smallest designs reported and suitable for integration into space-constrained devices. Its simple geometry enables easy design and integration across platforms. Frequency reconfigurability is achieved using PIN-diode-controlled reactive elements that manipulate current distribution to shift resonant frequencies. The design and optimization were performed using CST Microwave Studio to ensure accurate electromagnetic performance. Simulation results demonstrate that the proposed design supports up to eight distinct operating modes, highlighting its versatile frequency-reconfigurable capability. Among these modes, some achieve excellent performance at specific frequency bands including Wi-Fi 6E/7 (2.4, 5 and 6 GHz) and 5G sub-6 GHz (3.5 GHz). These findings are confirmed with simulation results showing clearly that the antenna exhibits S_11 below –20 dB across the targeted frequency bands. The antenna also demonstrates satisfactory gain, with values above 1.5 dBi across the desired frequency bands. The antenna reveals a voltage standing wave ratio (VSWR) below 1.5 across the intended frequency bands. These characteristics make the proposed antenna a compact, versatile and efficient solution for current and future wireless communication systems.

Corresponding Author:

Ismahane Refsi
Laboratory of Coding and Security of Information, Faculty of Electrical Engineering
University of Sciences and Technology of Oran Mohamed Boudiaf
31000, Oran, Algeria
Email: ismahane.refsi@univ-usto.dz

1. INTRODUCTION

In the context of rapidly evolving technology and the increasing demand for connected objects [1]-[4], wireless communication systems are constantly evolving to provide higher data rates, better energy efficiency and broad application integration. [5]. Hence, the fifth generation (5G) of mobile communication networks appears suitable to tailor these requirements in particular in the sub-6 GHz frequencies. Furthermore, the deployment of 5G [6] involves the cohabitation with other services in particular with those derived from the local-area network (WLAN) [7]. To tailor this exponential demand [8], a promising approach is the development of multi-standard antennas supporting 5G and Wi-Fi 6E/7, while addressing space constraints in smartphones and improving cost and energy efficiency [9]. Therefore, the antenna design must balance compactness with efficient multi-band performance [10]. The sub-6 GHz frequency range supports modern wireless applications with robust connectivity, fast speeds, and low latency, though it offers slightly lower data rates than millimeter-wave bands. This paper focuses on frequency reconfigurable antennas for sub-6 GHz applications.

Reconfigurability refers to the ability to adjust and adapt the radiation pattern, polarization and resonant frequency [11]. One or more mechanisms can be integrated into the same antenna [12] and the most suitable mechanism for the antenna design depends on the desired functionalities and properties [12]. Indeed, the reconfigurable antenna can be implemented in various applications including cognitive radio, multiple input-multiple-output (MIMO), satellites and wireless communication [13], [11]. In the mono-reconfiguration approach, three main types of antennas are identified: (i) frequency-reconfigurable antenna, (ii) pattern-reconfigurable antenna and (iii) polarization-reconfigurable antenna. Hussain *et al.* [14], a 4-element annular slot-based MIMO system integrated within Ultra-Wide Band (UWB) is introduced. However, this design suffers from a relatively large footprint of 60×120×1.5 mm, which limits its suitability for compact, space-constrained devices. The design of an asymmetric I-shaped dual broadband microstrip patch antenna with notch-based frequency reconfiguration is presented in [15]. However, the design is limited to only two operating bands and occupies a relatively large footprint of 39.6×47.6×1.6 mm that restricts its applicability in compact, multiband systems. Kumar *et al.* [16], the authors consider the design of a new A-shaped UWB antenna, operating over only a single frequency band. Tawk *et al.* [17], a novel approach to frequency reconfigurable antenna dual-band design using photoconductive silicon elements as optical switches is investigated but the design suffers from a large footprint and supports only two frequency bands. Bharathi and Gosula [18], a MIMO antenna design that is distinguished by its ability to operate in both triple and dual bands for WLAN applications is introduced. Even though the antenna operates in tri-bands, all bands are dedicated to WLAN applications with no 5G support. Moreover, it has a relatively large footprint (77.5×55.1×1.6 mm). Ghaffar *et al.* [19], the design and implementation of a compact frequency-reconfigurable multi-band antenna is presented, with a footprint of 30×15×1.6 mm. Dildar *et al.* [20], the authors introduce a frequency-reconfigurable antenna designed for IoT applications in 5G and sub-6 GHz wireless. However, it has a relatively large footprint 40×32×1.6 mm. Reconfigurable antennas offer the possibility to dynamically modify their radiation pattern, allowing them to adapt to different operating conditions and environments. This can result in improved signal quality and coverage [21]. Polarization reconfigurable antennas significantly reduce multipath fading. Most research into polarization reconfigurable antennas focuses on switching between right and left circular polarization at a specific frequency. In generals, electrical control devices such as PIN diodes or RF-MEMS are used [22].

Based on the previously cited methods, coplanar waveguide (CPW) structures have been widely used for broadband antennas due to their low signal distortion, minimal radiation loss and ease of fabrication. Building upon the cited designs and addressing their limitations, in this paper we present a compact FR4-based CPW-fed reconfigurable antenna tailored for multi-standard wireless applications, including Wi-Fi 6E/7, 5G sub-6 GHz and IoT, which are becoming increasingly essential in modern communication systems. The proposed antenna is one of the smallest reported in the literature, with overall dimensions of 28×15×1.6 mm, making it highly suitable for integration into space-constrained devices such as smartphones, wearable electronics and IoT modules. The antenna is capable of covering eight distinct operating modes, simultaneously supporting Wi-Fi 6E/7 and sub-6 GHz 5G, providing flexibility and adaptability for multi-standard wireless communications. The design adopts simple geometric shapes, which not only simplifies the analysis and optimization processes but also facilitates adaptation to different platforms unlike some of the cited methods that are often more complex and challenging to implement. Three PIN diodes are strategically employed to enable dynamic reconfiguration of the resonant behavior across the eight modes, allowing the antenna to adjust its frequency response according to specific application requirements. Furthermore, the use of an FR4 substrate combined with the simple geometry contributes to cost-effective fabrication, reducing production expenses compared to many of the previously reported designs. This approach addresses the limitations of cited methods that are relatively large or complex while ensuring efficient radiation performance, broad bandwidth coverage and ease of integration in compact wireless devices. Overall, the proposed antenna offers a promising solution for modern multi-standard wireless systems, combining compact size, simplicity, reconfigurability and cost efficiency, which are critical factors for next-generation communication technologies. Simulation results confirm its ability to provide satisfactory impedance matching, satisfactory gain and stable performance. In particular, the antenna demonstrates multi-band operation at 2.4–2.6 GHz, 3.1–3.8 GHz, 4.9–5.5 GHz, 6.0–6.8 GHz, and up to 7.3 GHz, which correspond to the targeted Wi-Fi (2.4/5/6 GHz), 5G sub-6 GHz, and ITU bands. These findings highlight the proposed antenna as a promising candidate for future multifunctional, reconfigurable and space-constrained wireless communication systems. The remainder of the paper is organized as follows. Section 2 introduces the followed methodology and the design of the proposed antenna. Section 3 presents the obtained results on the conducted experiments. Section 4 compares the obtained results with those of several state-of-the-art antennas. Finally, section 5 concludes this paper.

2. CONSIDRED METHODOLOGY AND ANTENNA DESIGN

2.1. General characteristics of designed antenna

Figure 1 illustrates the geometry of the proposed frequency-reconfigurable antenna, including its top and bottom. As it can be seen, the design is based on simple geometric forms, which helps to reduce fabrication complexity and facilitates low-cost manufacturing compared to some existing antenna. The geometry of the proposed antenna is fed by a CPW line. Figure 1(a) shows the top view, where the CPW conductor is connected to the rectangular patch. The CPW feed is divided into two sections, denoted as CPW_1 and CPW_2. Each section is characterized by its length L_{CPW} and width W_{CPW} which define the impedance of the feeding line and ensure proper matching with the radiating patch. Figure 1(b) presents the side view of the antenna geometry, while Figure 1(c) shows the bottom view with the arrangement of the metallic via pads. The antenna is implemented on an FR4-epoxy dielectric substrate ($\varepsilon_r = 4.4$, $\delta = 0.002, h = 1.6\,mm$) with a compact overall size of 25 × 18 × 1.6 mm. The use of FR-4 is dictated by its low cost, ease of fabrication and suitable electrical. The bottom layer hosts a rectangular patch that forms the main radiator of the antenna. To achieve frequency reconfigurability, both the left and right edges of this rectangular patch are connected to I-shaped extensions through PIN diodes. By selectively activating these diodes, additional current paths are created, which broaden the operating bandwidth and enable coverage of sub-6 GHz 5G frequency bands. Furthermore, an inverted L-shaped patch is positioned at the center of the structure and connected via a third PIN diode. This element further extends the resonance capabilities of the antenna. Metallic vias are employed to connect different layers of the structure ensuring stable electrical.

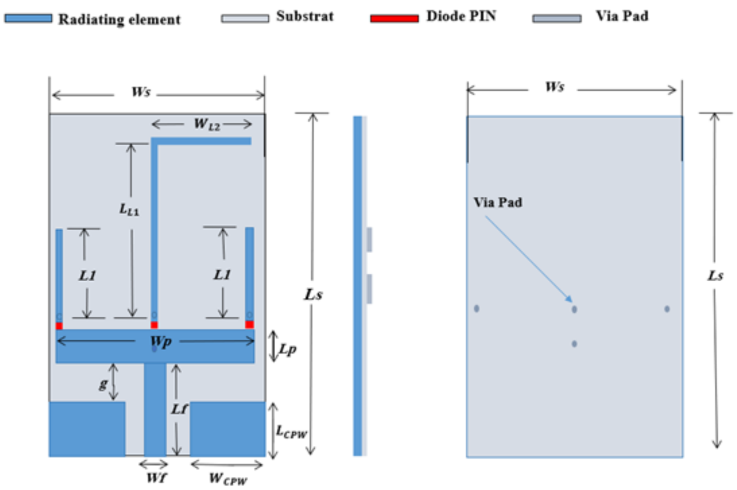

(a) (b) (c)

Figure 1. Geometry of the proposed reconfigurable antenna; (a) top view, (b) side view, and (c) bottom view

2.2. Design methodology

This subsection outlines the design procedure of the proposed antenna, which is based on a conventional monopole antenna due to its simple structure and efficient radiation characteristics. As observed in Figure 2, the proposed antenna is characterized by a simple and compact geometry, mainly composed of basic rectangular and linear elements. Such a structure not only simplifies the design process but also ensures ease of manufacturing. The reduced complexity minimizes fabrication errors and enhances reproducibility, making the antenna highly suitable for large-scale production. The initial structure consists of a rectangular patch placed on the bottom layer of the FR4 substrate and fed CPW as shown in Figure 2(a). From the literature review, the FR-4 is chosen for its efficient radiation properties, ease of integration with other RF components and simple fabrication process. The CPW is chosen as the feeding technique because it offers improved radiation characteristics. CPW feeding is advantageous for antenna design, offering a wide operating bandwidth, low dispersion and simplified construction. It also facilitates easy surface mounting of additional circuit components without the need for wraparound or via holes. The rectangular patch is defined by two geometrical parameters: its length L_P and its width W_P. These parameters constitute the fundamental dimensions of the monopole radiator and were optimized to ensure proper integration with the feeding structure. Given the overall antenna width of 15 mm, the rectangular radiator inside is set to approximately 14 mm to maintain a lateral clearance of about 0.5 mm on each side. This margin prevents unintended contact with the antenna boundary. The rectangular radiator is dimensioned to achieve a quarter-wavelength resonance around 5.2 GHz, which was the initial target frequency of the rectangular patch to effectively cover the Wi-Fi band. L_T is the total effective length of the monopole, defined in (1):

$$L_T = L_P + g \tag{1}$$

where L_P represents the physical length of the monopole radiator and $g$denotes the gap between the radiator and the CPW feed line. L_T can be calculated in (2):

$$L_T = \frac{c}{4f_0\sqrt{\varepsilon_\varepsilon}} \tag{2}$$

here $c = 3 \times 10^8\ m/s$ denotes the speed of light in free space and f_0 the central resonant frequency, chosen as 5.2 GHz. The term ε_ε represents the effective dielectric constant, which must be used instead of the relative permittivity ε_r [19].

Figure 3 illustrates the simulated result of S_{11} loss parameters of the rectangular monopole showing a clear resonance at 5.2 GHz corresponding to the targeted Wi-Fi band. The return loss at this frequency is below −10 dB, confirming the effectiveness of the rectangular radiator and demonstrates the suitability of the proposed antenna design for Wi-Fi applications. The second step of the design process extends the antenna operation to the sub-6 GHz 5G bands, with a focus on the 3.5 GHz band. To achieve this, sleeve structures are incorporated into the radiating patch, a widely adopted technique for lowering the resonant frequency and enabling antenna miniaturization. As a result, the initial resonant frequency of 5 GHz is shifted to 3.5 GHz by integrating two I-shaped stubs on both sides of the rectangular radiator. This configuration offers two main advantages: (1) it enables the excitation of additional resonant modes, thereby extending the antenna's operational bandwidth, and (2) the I-shaped stubs preserve a simple geometry, ensuring ease of fabrication and low production cost. The second step of the design process is illustrated in Figure 2(b). Each I-shaped stub exhibits the following dimension: length L_I and width W_I. The final step of the design introduces an additional resonance corresponding to the 2.4 GHz Wi-Fi band. To achieve this, an additional sleeve is incorporated at the center of the antenna. Based on the literature, F-shaped and L-shaped structures are commonly used as simple and effective solutions for generating lower-frequency resonances. In this work, an L-shaped stub is selected due to its structural simplicity and ease of fabrication. Figure 2(c) shows the final configuration of the proposed antenna. The inverted-L shaped strip is characterized by two main geometrical parameters: (1) the vertical section, referred to the *leg* of the L, with length L_{L1} and width W_{L1} and (2) the horizontal section, referred to the *base* of the L, with length L_{L2} and width W_{L1}.

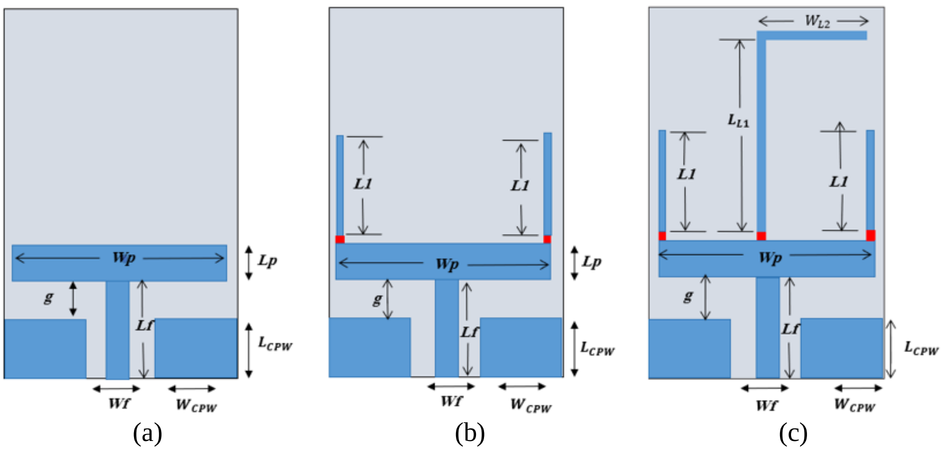

Figure 2. Design evolution of the proposed antenna; (a) initial antenna configuration with a rectangular radiator fed by a CPW line, (b) geometry of the antenna in the second design step, and (c) final geometry of the proposed antenna design

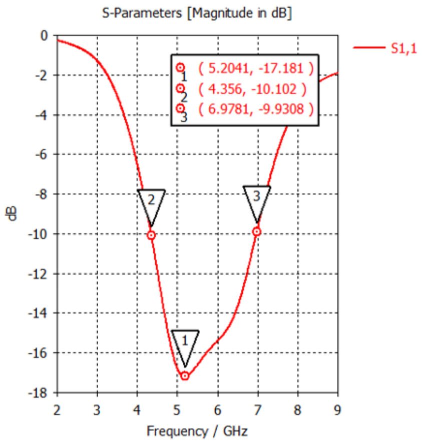

Figure 3. Simulated $|S_{11}|$ of the rectangular monopole

Figure 4 shows the equivalent electrical circuit of the PIN diode. A 50-Ω SMA connector was utilized to excite the structure while limiting its influence on the antenna characteristics. The HPND-4005 diode was implemented using a lumped RLC equivalent circuit. In the ON state Figure 4(a), the diode behaves as a series combination of a 0.15 nH inductor and a 4.7 Ω resistor. In contrast, in the OFF-state Figure 4(b), it is modeled as an inductor of 0.15 nH in series with a parallel network composed of a 0.017 pF capacitor and a 7 kΩ resistor. The equivalent model along with the biasing circuit is illustrated in Figure 4(c).

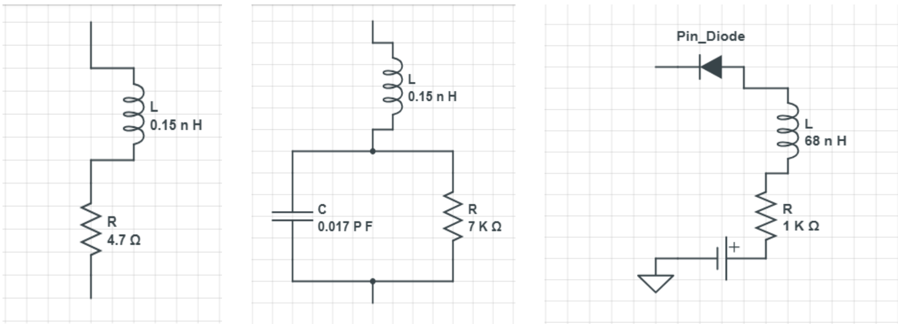

(a) (b) (c)

Figure 4. Equivalent electrical circuit of pin diode in (a) On state, (b) Off-state and (c) Electrical model of biasing circuit

Table 1 summarizes the optimized dimensions of the proposed antenna, including the CPW feed, rectangular patch, I-shaped patch, and inverted L-shaped patch.

Table 1. Optimized dimensions of the proposed antenna

Component	Characteristic	Dimension (mm)
CPW feed	L_{CPW}	3.5
	W_{CPW}	6
Rectangular patch	L_P	3.5
	W_P	14
I shaped patch	L_I	9.5
	W	1
L inverted shaped patch	L_{L1}	14
	W_{L1}	1
	L_{L2}	1
	W_{L2}	6.5

3. RESULTS AND DISCUSSION

This section presents the results obtained from the conducted simulations, evaluated through key performance parameters including return loss, gain, directivity and voltage standing wave ratio (VSWR). All simulations were carried out using CST Studio Suite, which provides a reliable framework for electromagnetic modeling and validation. The antenna is simulated using CST Studio Suite. Open (add space) boundary conditions are applied to emulate free-space radiation, with an added space of $\lambda/_4$ around the structure 31 mm. The time-domain solver is used with a hexahedral mesh.

3.1. Return loss (S-parameters)

Figure 5 presents the simulated return loss (S_{11}) for all configurations, illustrating the distinct resonant modes achieved through reconfiguration. This figure clearly highlights the impact of each switching state on the antenna's resonant behavior. To describe the multiple operating modes of the proposed antenna, a binary notation is adopted where '1' and '0' denote the ON and OFF states of the PIN diodes, respectively. This convention enables clear identification of the eight possible configurations, with case '000' corresponding to all diodes in the OFF state.

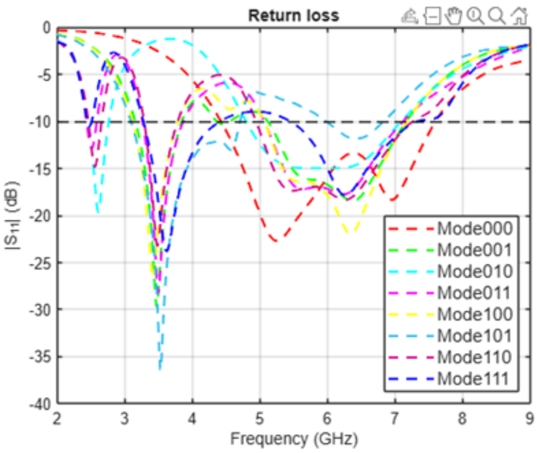

Figure 5. Return loss comparison among various diode states

The following describes the antenna behaviour for each mode. The following described the antenna behaviour for each mode.

- Case '000': when all diodes are in the OFF state, the antenna operates over a wide frequency range from 4.3 to 8.14 GHz, with a clear resonance at 5.2 GHz suitable for Wi-Fi applications. This result confirms that the considered monopole antenna effectively resonates at the targeted frequency. Moreover, it achieves satisfactory impedance matching, with an S_{11}value around −22.55 dB. An additional resonance around 7 GHz enables coverage of the ITU band and extended wireless services.
- Case '001': this configuration exhibits a resonance around 3.5 GHz, making it suitable for sub-6 GHz 5G applications. It achieves a bandwidth ranging from 3.16 to 3.8 GHz, with excellent impedance matching characterized by an S_{11} value of −27.54 dB. This behavior is attributed to the incorporation of I-shaped sleeves, which effectively reduce the resonant frequency of the monopole antenna by modifying the current path, thereby enabling operation at lower frequencies. In addition, a second resonance is observed around 6.5 GHz, covering Wi-Fi 6E/7 bands, with a wide bandwidth extending from 5.12 to 7.71 GHz and an S_{11} of −17.96 dB.
- Case '010': this configuration is dedicated to Wi-Fi applications, with resonances at 2.4 GHz (2.46–2.74 GHz, S_{11} arround −19.64 dB) and 5.2 GHz (S_{11} arround −14.38 dB), along with an additional resonance around 6 GHz for Wi-Fi 6E/7. This behavior is mainly due to the inverted L-shaped strip, which increases the effective current path length, thereby lowering the resonant frequency and enabling operation at 2.4 GHz, suitable for long-range Wi-Fi applications, while demonstrating that the addition of sleeves to the monopole is a simple and effective approach for frequency tuning.
- Case '011': multi-band operation is achieved with resonances at 2.4 GHz, 3.5 GHz, and between 5 GHz and 6 GHz. These bands support Wi-Fi, sub-6 GHz 5G and extended Wi-Fi applications, demonstrating high versatility.

- Case ‘100’: its behavior is generally similar to that observed in case ‘001’ with S_{11} arround −26.27 dB for the 3.4 GHz frequency.
- Case ‘101’: similar to Case ‘001’, this mode exhibits good return loss around 3.5 GHz, ensuring effective sub-6 GHz 5G operation.
- Case ‘110’: this mode is particularly suitable for 5G applications. This configuration exhibits three resonant modes around 2.58 GHz (S_{11} around −14.14 dB), 3.48 GHz (S_{11} around −23.13 dB), and 5.2 GHz (S_{11} around −16.38 dB), supporting Wi-Fi and sub-6 GHz 5G applications.
- Case ‘111’: strong resonances are observed at 3.5 GHz and within the 6–7 GHz range. This mode supports sub-6 GHz 5G and advanced Wi-Fi standards (Wi-Fi 6E/7), meeting next-generation wireless system requirements.

The results summarized in Table 2 clearly highlight the versatility of the proposed antenna. Depending on the switching configuration, the antenna is capable of operating in, single, dual- or tri-band modes, efficiently covering the most relevant wireless standards. In particular, resonances are achieved at 2.4 GHz (Wi-Fi), 3.5 GHz (5G sub-6 GHz), 5 GHz (Wi-Fi), and between 6–7 GHz (Wi-Fi 6E/7 and emerging 5G bands) as well as around 7 GHz, which corresponds to the ITU band. This confirms that the antenna offers high reconfigurability while maintaining a compact and simple geometry.

Table 2. Summary of the simulated spectral bands for the proposed antenna under different switching configurations, multi-standard communication systems

Switching mode	Operational mode	Resonance frequency (GHz)	Simulated bands (GHz)
000	Wideband	5.2	4.34-8.14
001	Dual-band	3.5, 6.5	3.1-4.71 and 6-6.8
010	Dual-band	2.4, 5.2	2.47-2.77 and 4.82-7.06
011	Tri-band	2.49, 3.5, 5.2	2.44-2.59, 3.26-3.86 and 5,09 -7.11
100	Dual-band	3.4, 5.2	3.11-3.78 and 5.07-7.17
101	Dual-band	3.5, 6.5	3.10-4.71 and 6-6.8
110	Tri-band	2.49, 3.4, 5.2	2.46-2.66,3.29-3.77 and 4.95-7.25
111	Tri-band	2.49, 3.5, 5.2	2.45-2.51, 3.29-4.38 and 5.45-7.32

3.2. Gain

Figure 6 represents the gain of the proposed antenna versus frequency over the 2-9 GHz band for the selected modes (negative-gain modes are omitted). The antenna reaches about 8-9 dBi at 2 GHz, then decreases around 3 GHz. Between 3 GHz and 9 GHz, the gain remains relatively stable, ranging from 2 dBi to 4 dBi with minimal variations, indicating good performance over a wide bandwidth.

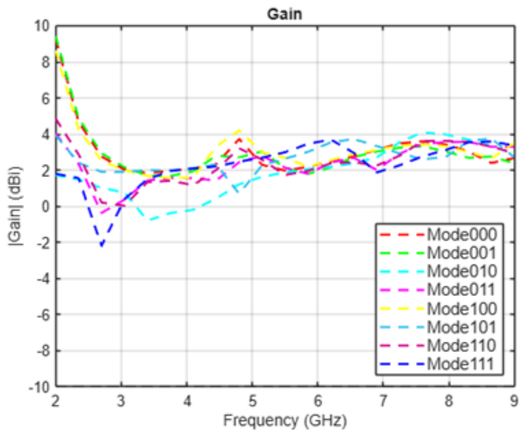

Figure 6. Gain comparison among various diode states

3.3. Directivity

Figure 7 shows the directivity of the proposed antenna versus frequency over the 2-9 GHz band for different operating modes. The results indicate that the directivity generally increases with frequency. At lower frequencies, it varies between 1.5 and 3 dBi. From 5 GHz to 9 GHz, higher values are achieved, reaching up to approximately 5-5.5 dBi for some modes, particularly Mode 111. Overall, the antenna exhibits improved directivity at higher frequencies with moderate variations between the different operating modes.

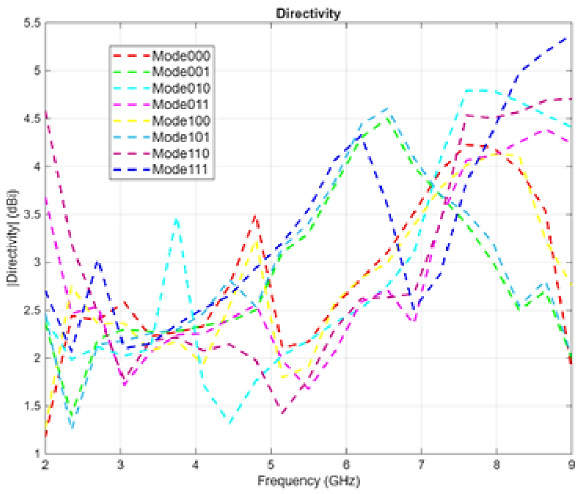

Figure 7. Directivity comparison among various diode states

3.3. VSWR

The VSWR is illustrated in Figure 8. The VSWR analysis shows that, for most modes, the values remain below 1.5. This indicates a satisfactory impedance matching of the antenna at its resonant frequencies, ensuring low reflection losses and adequate radiation efficiency.

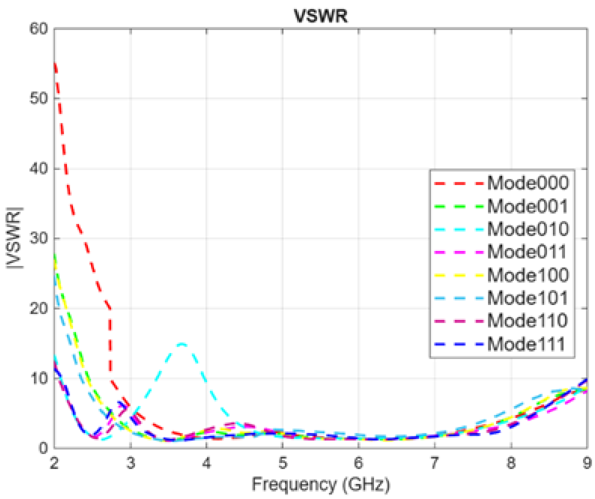

Figure 8. VSWR comparison among various diode states

4. PERFORMANCE COMPRAISON

Table 3 presents a comparison between the proposed antenna and other state-of-the-art works for similar applications. The proposed antenna stands out by offering a smaller size than the cited works and supporting a larger number of operating bands. In addition, it features a simple and thin geometry, mainly due to the CPW feeding technique, where the central conductor and the ground planes are placed on the same side of the substrate. This configuration not only simplifies the design but also enhances integration with modern circuits. In contrast, several reported designs rely on complex or moderately intricate structures to achieve comparable or even inferior results. Moreover, the proposed antenna represents a promising solution for modern wireless communication systems, as it covers both traditional Wi-Fi bands (2.4 and 5 GHz) and the latest standards, including Wi-Fi 6E, Wi-Fi 7 and sub-6 GHz 5G.

Table 3. Performance comparison of the proposed antenna with state-of-the-art works

Works	Operational region (GHz)	Principals' frequencies (GHz)	Dimensions (mm^2)	NO. of switches	Operational bands per mode	Number of bands
[19]	2 – 9	2.4, 3.5, 5.2	15 × 30	3 PIN diodes	Single, dual, tri, wideband	12
[23]	2 – 8	2.4, 3.5, 4.7, 5.8	35 × 35	3 PIN diodes	Single, dual	5
[24]	2.9 – 5.32	3, 4.2, 4.6, 5.2	25.34 × 25.33	2 Varactor diodes	Single, tri	4
[25]	2 – 6	0.988, 2.67, 3.36, 4.58, 4.76, 4	80 × 80	2 PIN diodes	Dual, triple, wideband	6
[26]	1 – 6	1.9,2.45,3,5.2,5.9	45 × 45	3 PIN diodes	Wideband	6
[27]	1 – 4	1.5,3.5,1.6,2,2.5,3	60 × 60	4 PIN diodes	Single, dualband	6
[28]	1 – 7	1.91–2.68, 3.3–3.75, 5.55–6.75	40 × 40	2 PIN diodes	Triple, wideband	3
	2 – 6	2.7, 3.6, 4.6, 4.8	30 × 20	2 PIN diodes	Single, dual, tripleband	4
Our work	2 – 9	2.4, 3.4, 3.5, 5.2	15 × 28	3 PIN diodes	Single, dual, tri, wideband	18

5. CONCLUSION

In this work, a compact frequency-reconfigurable antenna suitable for multi-standard wireless communication systems has been proposed and analyzed. The antenna is designed on an FR4 substrate with dimensions of 28 mm×15 mm×1.6 mm and fed by a CPW structure to ensure ease of integration and efficient radiation. By employing three PIN diodes, the antenna achieves eight distinct reconfiguration modes, allowing it to dynamically adapt to different wireless standards. Simulation results confirm that the antenna covers several key frequency bands, including 2.4 GHz (Wi-Fi), 3.5 GHz (5G sub-6 GHz), 5.2/5.5 GHz (Wi-Fi), 6–6.8 GHz (Wi-Fi 6E/7) and up to 7.3 GHz (ITU band). The proposed design therefore demonstrates versatility and robustness, while maintaining compactness, low cost and ease of fabrication through the use of simple geometric structures. According to its performance and reconfigurability, the antenna stands as a strong candidate for integration into future multifunctional wireless platforms, such as smartphones, IoT devices, and emerging 5G/6G systems, where space, cost, and flexibility are critical factors. Thus, this antenna design can reduce the need for multiple antennas in smartphones, lowering cost and improving energy efficiency. As a future improvement, the antenna will be further miniaturized by reducing the number of PIN diodes to a single switching element. This modification aims to decrease the overall size and complexity of the structure while preserving similar resonant characteristics and maintaining comparable performance in terms of operating frequency bands and impedance matching. Future work and perspectives include the integration of the proposed antenna into MIMO systems to enhance overall system performance. Additionally, the design could be fabricated using advanced substrates such as Rogers materials or flexible substrates to further improve performance and adaptability. Finally, experimental validation in real-world applications such as smartphones or IoT modules is recommended to assess practical feasibility and performance.

FUNDING INFORMATION

Authors state no funding involved.

AUTHOR CONTRIBUTIONS STATEMENT

This journal uses the Contributor Roles Taxonomy (CRediT) to recognize individual author contributions, reduce authorship disputes, and facilitate collaboration.

Name of Author	C	M	So	Va	Fo	I	R	D	O	E	Vi	Su	P	Fu
Ismahane Refsi	✓	✓	✓	✓	✓	✓	✓	✓	✓	✓	✓			
Miloud Benchehima	✓	✓		✓	✓	✓	✓		✓	✓	✓	✓	✓	
Mohammed Hicham Hachemi	✓			✓		✓								
Salah Eddine Brezini	✓		✓	✓	✓				✓	✓	✓			

C : **C**onceptualization
M : **M**ethodology
So : **So**ftware
Va : **Va**lidation
Fo : **Fo**rmal analysis
I : **I**nvestigation
R : **R**esources
D : **D**ata Curation
O : Writing - **O**riginal Draft
E : Writing - Review & **E**diting
Vi : **Vi**sualization
Su : **Su**pervision
P : **P**roject administration
Fu : **Fu**nding acquisition

CONFLICT OF INTEREST STATEMENT

We have no conflicts of interest to disclose.

DATA AVAILABILITY

Data availability is not applicable to this paper as no new data were created or analyzed in this study.

REFERENCES

[1] A. Souri, A. Hussien, M. Hoseyninezhad, and M. Norouzi, "A systematic review of IoT communication strategies for an efficient smart environment," *Transactions on Emerging Telecommunications Technologies*, vol. 33, no. 3, Mar. 2022, doi: 10.1002/ett.3736.

[2] E. M. Ali, W. A. Awan, A. Abbas, S. M. Abbas, and H. G. Mohamed, "Compact frequency-agile and mode-reconfigurable antenna for C-Band, Sub-6-GHz-5G, and ISM applications," *Micromachines*, vol. 16, no. 6, p. 724, Jun. 2025, doi: 10.3390/mi16060724.

[3] M. H. Alsharif and R. Nordin, "Evolution towards fifth generation (5G) wireless networks: Current trends and challenges in the deployment of millimetre wave, massive MIMO, and small cells," *Telecommunication Systems*, vol. 64, no. 4, pp. 617-637, Apr. 2017, doi: 10.1007/s11235-016-0195-x.

[4] G. A. Akpakwu, B. J. Silva, G. P. Hancke, and A. M. Abu-Mahfouz, "A survey on 5G networks for the internet of things: communication technologies and challenges," *IEEE Access*, vol. 6, pp. 3619–3647, 2017, doi: 10.1109/ACCESS.2017.2779844.

[5] R. Alhamad, E. Almajali, and S. Mahmoud, "Electrical reconfigurability in modern 4G, 4G/5G and 5G antennas: a critical review of polarization and frequency reconfigurable designs," *IEEE Access*, vol. 11, pp. 29215-29233, 2023, doi: 10.1109/ACCESS.2023.3260073.

[6] P. Chen, X. Wang, D. Wang, Z. Gan, Y. Yin, and H. Zhang, "A frequency and beamwidth reconfigurable antenna based on liquid crystal for 5G millimeter waves," *Scientific Reports*, vol. 15, no. 1, p. 17822, May 2025, doi: 10.1038/s41598-025-01673-0.

[7] M. Ikram, E. Al Abbas, N. Nguyen-Trong, K. H. Sayidmarie, and A. Abbosh, "Integrated frequency-reconfigurable slot antenna and connected slot antenna array for 4G and 5G mobile handsets," *IEEE Transactions on Antennas and Propagation*, vol. 67, no. 12, pp. 7225-7233, Dec. 2019, doi: 10.1109/TAP.2019.2930119.

[8] I. Ahmad *et al.*, "Frequency reconfigurable antenna for multi standard wireless and mobile communication systems," *Computers, Materials and Continua*, vol. 68, no. 2, pp. 2563-2578, 2021, doi: 10.32604/cmc.2021.016813.

[9] J. M. Hannula, T. Saarinen, J. Holopainen, and V. Viikari, "Frequency reconfigurable multiband handset antenna based on a multichannel transceiver," *IEEE Transactions on Antennas and Propagation*, vol. 65, no. 9, pp. 4452-4460, Sep. 2017, doi: 10.1109/TAP.2017.2725384.

[10] C. G. Christodoulou, Y. Tawk, S. A. Lane, and S. R. Erwin, "Reconfigurable antennas for wireless and space applications," *Proceedings of the IEEE*, vol. 100, no. 7, pp. 2250–2261, Jul. 2012, doi: 10.1109/JPROC.2012.2188249.

[11] T. Tandel and S. Trapasiya, "Reconfigurable antenna for wireless communication: recent developments, challenges and future," *Wireless Personal Communications*, vol. 133, no. 2, pp. 725-768, Nov. 2023, doi: 10.1007/s11277-023-10785-7.

[12] J. Costantine, Y. Tawk, S. E. Barbin, and C. G. Christodoulou, "Reconfigurable antennas: design and applications," *Proceedings of the IEEE*, vol. 103, no. 3, pp. 424–437, Mar. 2015, doi: 10.1109/JPROC.2015.2396000.

[13] Q. U. A. Nadeem, A. Kammoun, M. Debbah, and M. S. Alouini, "Design of 5G full dimension massive MIMO systems," *IEEE Transactions on Communications*, vol. 66, no. 2, pp. 726-740, Feb. 2018, doi: 10.1109/TCOMM.2017.2762685.

[14] R. Hussain, M. S. Sharawi, and A. Shamim, "An Integrated four-element slot-based MIMO and a UWB sensing antenna system for CR platforms," *IEEE Transactions on Antennas and Propagation*, vol. 66, no. 2, pp. 978-983, Feb. 2018, doi: 10.1109/TAP.2017.2781220.

[15] R. K. Verma, D. K. Srivastava, R. P. Tripathi, and V. Rajpoot, "Wide dual band asymmetrical i-shape rectangular microstrip patch antenna for PCS/UMTS/WiMAX/IMT applications," *Wireless Personal Communications*, vol. 122, no. 2, pp. 1577-1598, Jan. 2022, doi: 10.1007/s11277-021-08962-7.

[16] P. Kumar, S. Shilpi, A. Kanungo, V. Gupta, and N. K. Gupta, "A novel ultra wideband antenna design and parameter tuning using hybrid optimization strategy," *Wireless Personal Communications*, vol. 122, no. 2, pp. 1129-1152, Jan. 2022, doi: 10.1007/s11277-021-08942-x.

[17] Y. Tawk, A. R. Albrecht, S. Hemmady, G. Balakrishnan, and C. G. Christodoulou, "Optically pumped frequency reconfigurable antenna design," *IEEE Antennas and Wireless Propagation Letters*, vol. 9, pp. 280-283, 2010, doi: 10.1109/LAWP.2010.2047373.

[18] A. Bharathi and R. S. R. Gosula, "A novel compact multiband reconfigurable WLAN MIMO antenna," *IETE Journal of Research*, vol. 69, no. 3, pp. 1466-1474, Apr. 2023, doi: 10.1080/03772063.2020.1869598.

[19] A. Ghaffar, X. J. Li, W. A. Awan, A. H. Nazeri, N. Hussain, and B. C. Seet, "Compact multiband multimode frequency reconfigurable antenna for heterogeneous wireless applications," *International Journal of RF and Microwave Computer-Aided Engineering*, vol. 31, no. 7, Jul. 2021, doi: 10.1002/mmce.22659.

[20] H. Dildar *et al.*, "Design and experimental analysis of multiband frequency reconfigurable antenna for 5G and Sub-6 GHz wireless communication," *Micromachines*, vol. 12, no. 1, p. 32, Dec. 2020, doi: 10.3390/mi12010032.

[21] B. Ahn, H. W. Jo, J. S. Yoo, J. W. Yu, and H. L. Lee, "Pattern reconfigurable high gain spherical dielectric resonator antenna operating on higher order mode," *IEEE Antennas and Wireless Propagation Letters*, vol. 18, no. 1, pp. 128-132, Jan. 2019, doi: 10.1109/LAWP.2018.2882871.

[22] K. Saraswat and A. R. Harish, "Dual-band polarisation reconfigurable grounded fractal slot antenna," *IET Microwaves, Antennas & Propagation*, vol. 14, no. 14, pp. 1786-1790, Nov. 2020, doi: 10.1049/iet-map.2020.0542.

[23] K. Thenkumari, K. S. Sankaran, and J. M. Mathana, "Design and implementation of frequency reconfigurable antenna for Wi-Fi applications," *Engineered Science*, vol. 23, 2023, doi: 10.30919/es8d876.

[24] M. Kurugodu Hanumanthappa and S. Mehta, "Frequency reconfigurable rectangular patch antenna for cognitive radio applications," *International Journal of Electrical and Computer Engineering (IJECE)*, vol. 13, no. 1, p. 579, Feb. 2023, doi: 10.11591/ijece.v13i1.pp579-589.

[25] K. Karthika and K. Kavitha, "Design and development of self-complementary DNA structure-based frequency reconfigurable antenna," *Journal of Electrical Engineering and Technology*, vol. 19, no. 8, pp. 5247-5258, Nov. 2024, doi: 10.1007/s42835-024-01917-5.

[26] V. Subashini, S. Chitra, and S. Ramesh, "Performance analysis of multiband frequency-reconfigurable antenna for cognitive radio applications," *Journal on Wireless Communications and Networking*, vol. 2026, no. 1, p. 5, Jan. 2026, doi: 10.1186/s13638-025-02555-9.
[27] A. A. Ibrahim, W. A. E. Ali, M. Alathbah, and H. A. Mohamed, "A frequency reconfigurable folded antenna for cognitive radio communication," *Micromachines*, vol. 14, no. 3, p. 527, Feb. 2023, doi: 10.3390/mi14030527.
[28] A. K. Singh *et al.*, "Low-loss paper-substrate triple-band-frequency reconfigurable microstrip antenna for Sub-7 GHz applications," *Sensors*, vol. 23, no. 21, p. 8996, Nov. 2023, doi: 10.3390/s23218996.

BIOGRAPHIES OF AUTHORS

Ismahane Refsi She received her bachelor's degree in electronics in 2017 and her master's degree in networks and telecommunications in 2019 from the University of Science and Technology of Oran–Mohamed Boudiaf (USTO-MB), Algeria. Since 2023, she has been a Ph.D. student and a member of the LACOSI laboratory at the University of Science and Technology of Oran–Mohamed Boudiaf (USTO-MB), Algeria. Her doctoral research focuses on LTE (4G), 5G, and beyond networks, cognitive radio, mobility management, quality of service optimization, and the design of reconfigurable antennas. She can be contacted at email: ismahane.refsi@univ-usto.dz.

Miloud Benchehima received his Ph.D. degree in electronics in 2016 at Sidi Bel Abbes' University, Algeria. Since 2017, he is senior lecturer at USTO-MB's University (Oran, Algeria) and he received HDR degree in the same field since 2021. His research interests are in: optical communication networks, computational materials science, semiconductor device modeling, optics and communication device and antennas. He can be contacted at email: miloud.benchehima@univ-usto.dz.

Mohammed Hicham Hachemi obtained his state engineer degree in telecommunications from the University of Saida, in 2007 (Algeria). He received his magister degree in Electronics from the Doctoral School of Sciences, Information Technology, and Telecommunications at University of Sidi Bel Abbes, in 2011 (Algeria) and Ph.D. in Telecommunications in 2017 at the UABT's University, Tlemcen (Algeria). Starting in 2017, he took on the role of senior lecturer and researcher at the USTO-MB's University, and was promoted to habilitated to direct research (HDR) in 2022 at the same University. His current research interests include artificial intelligence, machine learning, deep learning, autonomous vehicles, cognitive radio, 5G and beyond, 6G, mobility management and design and analysis of 5G and beyond antennas. He can be contacted at email: hicham.hachemi@univ-usto.dz.

Salah Eddine Brezini He received his bachelor's degree in telecommunications in 2015 and his master's degree in networks and telecommunications, with a focus on signal and image processing, in 2017. In 2022, he obtained his Ph.D. degree in signal and image processing from Université Paul Sabatier Toulouse III, France, co-supervised with the University of Science and Technology of Oran–Mohamed Boudiaf (USTO-MB), Algeria. Since 2022, he has been a faculty member and researcher at USTO-MB. His research interests include linear and nonlinear spectral/spatial unmixing techniques in remote sensing imagery, including statistical and blind source separation (BSS) methods with applications to remote sensing, and the design of reconfigurable antennas. He can be contacted at email: salaheddine.brezini@univ-usto.dz.